

# Nck-dependent Activation of Extracellular Signal-regulated Kinase-1 and Regulation of Cell Survival during Endoplasmic Reticulum Stress<sup>□</sup>

Duc Thang Nguyen,\* Sem Kebache,<sup>†</sup> Ali Fazel,<sup>‡</sup> Hetty N. Wong,<sup>§</sup>  
Sarah Jenna,<sup>||</sup> Anouk Emadali,\* Eun-hye Lee,<sup>||</sup> John J.M. Bergeron,<sup>‡||</sup>  
Randal J. Kaufman,<sup>§</sup> Louise Larose,<sup>†</sup> and Eric Chevet\*<sup>‡||¶</sup>

Departments of \*Surgery, <sup>†</sup>Experimental Medicine, and <sup>‡</sup>Anatomy and Cell Biology, <sup>||</sup>Montreal Proteomic Network, McGill University, Montreal, Quebec, H3A 1A1 Canada; and <sup>§</sup>Department of Biological Chemistry, Howard Hughes Medical Institute, University of Michigan Medical School, Ann Arbor, MI 48109-0650

Submitted November 26, 2003; Revised May 21, 2004; Accepted June 7, 2004  
Monitoring Editor: Jennifer Lippincott-Schwartz

In response to stress, the endoplasmic reticulum (ER) signaling machinery triggers the inhibition of protein synthesis and up-regulation of genes whose products are involved in protein folding, cell cycle exit, and/or apoptosis. We demonstrate that the misfolding agents azetidine-2-carboxylic acid (Azc) and tunicamycin initiate signaling from the ER, resulting in the activation of Jun-N-terminal kinase, p44<sup>MAPK</sup>/extracellular signal-regulated kinase-1 (ERK-1), and p38<sup>MAPK</sup> through IRE1 $\alpha$ -dependent mechanisms. To characterize the ER proximal signaling events involved, immuno-isolated ER membranes from rat fibroblasts treated with ER stress inducers were used to reconstitute the activation of the stress-activated protein kinase/mitogen-activate protein kinase (MAPK) pathways *in vitro*. This allowed us to demonstrate a role for the SH2/SH3 domain containing adaptor Nck in ERK-1 activation after Azc treatment. We also show both *in vitro* and *in vivo* that under basal conditions ER-associated Nck represses ERK-1 activation and that upon ER stress this pool of Nck dissociates from the ER membrane to allow ERK-1 activation. Moreover, under the same conditions, Nck-null cells elicit a stronger ERK-1 activation in response to Azc stress, thus, correlating with an enhanced survival phenotype. These data delineate a novel mechanism for the regulation of ER stress signaling to the MAPK pathway and demonstrate a critical role for Nck in ER stress and cell survival.

## INTRODUCTION

The endoplasmic reticulum (ER) is the subcellular compartment where secretory proteins acquire their correct conformation after entering the secretory pathway. When proteins cannot achieve their correct folding due to mutations (Aridor and Balch, 1999; High *et al.*, 2000) or due to changes in the ER luminal environment, they accumulate and ultimately aggregate within this compartment (Kaufman, 1999). As a consequence, the unfolded protein response (UPR) is triggered in the ER to counterbalance proteotoxicity. This phenomenon is associated with the induction of specific genes (Kaufman, 1999; Zhang and Kaufman, 2004) that encode specific ER resident molecular chaperones that aid protein folding (Kaufman, 1999), or proteins that are in-

involved in ER-associated degradation (Yoshida *et al.*, 2003), as well as transcription factors such as GADD153/CHOP (Wang *et al.*, 1998) and XBP-1 (Yoshida *et al.*, 2001).

In mammalian cells, UPR induction is mainly mediated by the ER resident transmembrane proteins IRE1 $\alpha$ , IRE1 $\beta$ , and ATF-6 (Haze *et al.*, 1999). IRE1 $\alpha$  is constitutively expressed, whereas IRE1 $\beta$  expression is restricted to specific cell types (Yoshida *et al.*, 2001; Calton *et al.*, 2002; Lee *et al.*, 2002). The cytosolic domains of IRE1 $\alpha$  and IRE1 $\beta$  have both kinase and endoribonuclease activities (Bork and Sander, 1993), whereas the cytosolic domain of ATF-6 acts as a transcription factor (Haze *et al.*, 1999). ATF6 and IRE1 synergize expression and splicing of the UPR-induced transcription factor XBP-1 (Yoshida *et al.*, 2001; Calton *et al.*, 2002; Lee *et al.*, 2002). In addition, it has been observed that the Jun-N-terminal kinase (JNK-1) is activated in response to ER stress. This is mediated through IRE1 binding to the scaffold molecule TRAF-2 (Urano *et al.*, 2000b) and the consequent docking and activation of ASK-1/JNK-1 (Nishitoh *et al.*, 2002). This signaling pathway is very similar to that downstream of tumor necrosis factor (TNF) receptors upon TNF activation (Chen *et al.*, 2002). The involvement of the mitogen-activate protein kinase (MAPK)/stress-activated protein kinase (SAPK) signaling pathways during ER stress has been further described with the activation of p38<sup>MAPK</sup> mediated by ATF-6 (Luo and Lee, 2002). It is well established that stress-mediated activation of the MAPK pathways is a gen-

Article published online ahead of print. Mol. Biol. Cell 10.1091/mbc.E03-11-0851. Article and publication date are available at [www.molbiolcell.org/cgi/doi/10.1091/mbc.E03-11-0851](http://www.molbiolcell.org/cgi/doi/10.1091/mbc.E03-11-0851).

□ Online version of this article contains supporting material. Online version is available at [www.molbiolcell.org](http://www.molbiolcell.org).

¶ Corresponding author. E-mail address: [eric.chevet@mcgill.ca](mailto:eric.chevet@mcgill.ca).

Abbreviations used: Azc, azetidine-2-carboxylic acid; CNX, calnexin; ER, endoplasmic reticulum; MAPK, mitogen-activated protein kinase; RLC, rat liver cytosol; SAPK, stress-activated protein kinase; Tun, tunicamycin; UPR, unfolded protein response.

eral mechanism by which cells respond to maintain their integrity (Johnson and Lapadat, 2002). In higher organisms, there are four subfamilies of MAPKs. They include extracellular signal-regulated kinase (ERK/MAPK) 1/2; c-Jun amino-terminal kinase (JNK/SAPK), and p38 and big mitogen-activated protein kinase/extracellular signal-regulated kinase (BMK-1/ERK-5) (Hazzalin and Mahadevan, 2002; Johnson and Lapadat, 2002). Depending on the stress, the activation of these kinases can either positively or negatively regulate the cell proliferative or apoptotic responses (Wada and Penninger, 2004). Although many scaffold proteins have been reported to participate in the MAPK signaling cascade (Morrison and Davis, 2003), to date only the adaptor molecule TRAF-2 has been described as being directly involved in the ER stress-induced MAPK activation (Urano *et al.*, 2000b).

Together, these observations led us to postulate that signaling from the ER membrane to downstream kinase pathways may occur in a manner similar to that which occurs at the plasma membrane after the binding of hormone/growth factor to membrane receptors. To test this hypothesis, we developed a cell-free assay that allowed us to demonstrate that the SH2/SH3 domain containing adaptor Nck regulates Azc-induced ER stress-mediated ERK-1 activation, thus providing evidence for the involvement of a novel signaling network that mediates stress signals from the ER.

## MATERIALS AND METHODS

### Cell Lines

FR3T3 fibroblasts were used as described previously (Chevet *et al.*, 1999a). IRE1 $\alpha^{+/+}$  mouse embryonic fibroblasts (MEFs) and IRE1 $\alpha^{-/-}$  MEFs were described previously (Yoshida *et al.*, 2001; Calfon *et al.*, 2002; Lee *et al.*, 2002). Nck $^{+/+}$  (Nck-1 $^{-/-}$  Nck-2 $^{+/+}$ ) and Nck $^{-/-}$  MEFs (Nck-1 $^{-/-}$  Nck-2 $^{-/-}$ ) were kindly provided by Friedhelm Bladt, Sigal Gelpok, and Anthony J. Pawson (Samuel Lunenfeld Research Institute, Mount Sinai Hospital, Toronto, Ontario, Canada) (Gruenheid *et al.*, 2001).

### Reagents

Anti-Calnexin (CNX)-C3 and -C4 antisera were used as described previously (Chevet *et al.*, 1999b). Anti-Nck antibodies were generated as described by Lussier and Larose (1997). Anti-MG-160 was a kind gift from Dr. N. K. Gonatas (University of Pennsylvania Medical Center, Philadelphia, PA), anti-Tom20 was kindly provided by Dr. G. Shore (McGill University, Montreal, PQ, Canada). Anti-IRE1 $\alpha$  and anti-IRE1 $\beta$  antibodies were kindly given by Dr. D. Ron (New York University, New York, NY). Anti-BiP antibodies were kindly provided by Dr. L. Hendershot (St. Jude Children's Research Hospital, Memphis, TN). Anti-Grb-2 antibodies were purchased from Upstate Biotechnology (Lake Placid, NY). Anti-ERK-1, anti-JNK-1, anti-p38<sup>MAPK</sup>, anti-phospho-p38<sup>MAPK</sup>, anti-phospho-JNK, and anti-Crk antibodies were purchased from Santa Cruz Biotechnology (Santa Cruz, CA). Anti-phospho-ERK antibodies were from BD Transduction Laboratories (Lexington, KY). Anti-myc antibodies were purchased from Cell Signaling Technology (Beverly, MA). Anti-rabbit IgG fluorescein isothiocyanate (FITC)-conjugate, anti-mouse IgG tetramethylrhodamine B isothiocyanate (TRITC)-conjugate, azetidine-2-carboxylic acid (Azc), and sodium arsenite (NaAs) were purchased from Sigma-Aldrich (St. Louis, MO) and tunicamycin (Tun) was from Calbiochem (San Diego, CA).

### DNA Constructs and Recombinant Proteins

Shc-SH2 and Shc-SH2 mutant chimeras were generated as described previously (Di Guglielmo *et al.*, 1994). Individual Nck-1 src homology (SH)3 domains fused to glutathione S-transferase (GST), Nck-1 SH3-1-GST, Nck-1 SH3-2-GST, and Nck-1 SH3-3-GST, were described previously (Kebache *et al.*, 2002). GST-IRE1 $\alpha$  and GST-IRE1 $\beta$  fusion proteins corresponded to the respective cytosolic domains N-terminally fused to GST. All the constructs were sequence verified. GST fusion proteins were cleaved by thrombin digestion, purified using benzamide-Sepharose chromatography, and concentrated on Centricon columns (Millipore, Bedford, MA). Nck-1(3SH3)wt and Nck-1(3SH3)dead were generated as described previously (Kebache *et al.*, 2002). IRE1 $\alpha$ .Nck-1 and Trap $\alpha$ .Nck-1 fusion proteins were generated as follows: DNA fragments encoding the luminal and transmembrane domains of IRE1 $\alpha$  (aa 1-555) or Trap $\alpha$  (aa 1-250) were polymerase chain reaction (PCR) amplified with High Fidelity polymerase (Invitrogen, Carlsbad, CA) by using the

following primers: 5'-CCCAAGCTTGGGATGCCGGCCCGG and 5'-CCCAAGCTTGGGCTTGTCCAGGGAGGG for IRE1 $\alpha$ ; and 5'-CGCGGATCCG-CATGAGACTCCTCCCCCG and 5'-CGCGGATCCGCGATCATTCTGACTT-GATGTACCATT for Trap $\alpha$ . Fragments were digested with either *Hind*III or *Bam*HI for IRE1 $\alpha$  and Trap $\alpha$  PCR products, respectively, and inserted in their respective restriction site, upstream of pcDNA3.Nck-1(full-length) (Kebache *et al.*, 2002). Positive clones were assessed by restriction mapping and sequencing.

### Cell Transfection and In Vivo MAPK Assays

FR3T3 cells were transfected with either pcDNA3, pcDNA3/IRE1 $\alpha$ .Nck-1 or pcDNA3/Trap $\alpha$ .Nck-1, by using Lipofectamine (Invitrogen). FR3T3-transfected cells, IRE1 $\alpha^{+/+}$  MEFs, IRE1 $\alpha^{-/-}$  MEFs, Nck $^{+/+}$  MEFs, and Nck $^{-/-}$  MEFs were treated with 10 mM Azc or 10  $\mu$ g/ml Tun for 10 min to 2 h. After treatment, cells were lysed in 20 mM Tris-HCl, pH 8.0, 150 mM NaCl, 1% Triton X (TX)-100, 1 mM NaF, 1 mM Na<sub>3</sub>VO<sub>4</sub>, 1 mM phenylmethylsulfonyl fluoride (PMSF), and 10  $\mu$ g/ml leupeptin and aprotinin (lysis buffer, LB). Lysates were resolved by SDS-PAGE and analyzed by immunoblot by using either anti-ERK-1, anti-p38<sup>MAPK</sup>, anti-JNK-1, anti-phospho-ERK, anti-phospho-p38<sup>MAPK</sup>, anti-phospho-JNK-1, or anti-CNX antibodies.

### Immuno-isolation of ER-enriched Membranes

Cells were stressed by incubation with either 10 mM Azc, 10  $\mu$ g/ml Tun, or 50  $\mu$ M NaAs for 10 min to 2 h. Membrane fractions were immunopurified as described previously (Lin *et al.*, 1999). Briefly, for immuno-isolation of the calnexin-enriched fraction, cells were grown on 15-cm dishes (5 plates/condition) under stress or nonstress conditions, scraped in 150 mM KCl, 10 mM Tris-HCl, pH 7.5, 2.5 mM MgOAc, 0.5 mg/ml bovine serum albumin (BSA), 0.25 M sucrose, 4 mM imidazole pH 7.4, containing 1 mM PMSF, 1  $\mu$ g/ml leupeptin, 1  $\mu$ g/ml aprotinin, 1 mM NaF, and 1 mM Na<sub>3</sub>VO<sub>4</sub> (homogenization buffer, HB), homogenized (30 strokes using a Teflon potter), and precleared. Postnuclear supernatants (PNS) were incubated either with affinity purified anti-CNX (C3+C4) antibodies cross-linked to M-280 magnetic beads (DynaL Biotech, Lake Success, NY) for 2-3 h at 4°C or with anti-CNX (C3+C4) antibodies followed by incubation with protein A-coupled magnetic beads (DynaL Biotech) for 1 h at 4°C with gentle rotation. Beads were isolated with a magnet, washed three times with HB, and two times with HB without BSA. The quality of the isolated membranes was assessed by immunoblotting and electron microscopy as described previously (Lavoie *et al.*, 2000).

### In Vitro Kinase Assays

Clarified lysates from FR3T3 cells treated either with 10 mM Azc, 10  $\mu$ g/ml Tun, or 50  $\mu$ M NaAs for 10 min to 2 h were immunoprecipitated with either anti-ERK-1, anti-p38<sup>MAPK</sup>, or anti-JNK-1 antibodies overnight at 4°C. Kinase reactions were then performed at 30°C for 20 min in kinase buffer (KB) (30 mM Tris-HCl, pH 8.0, 10 mM MgCl<sub>2</sub>, 1 mM NaF, and 1 mM Na<sub>3</sub>VO<sub>4</sub>) supplemented with 10  $\mu$ Ci of [ $\gamma$ -<sup>32</sup>P]ATP and 0.1 mM ATP and 2  $\mu$ g of myelin basic protein or 2  $\mu$ g of GST-ATF-2 or 2  $\mu$ g of GST-JUN. Reactions were collected and analyzed by SDS-PAGE and autoradiography.

### Cell-Free Activation of MAPK/SAPK Pathways

Three milligrams of rat liver cytosol (RLC) were incubated with 30  $\mu$ g of FR3T3-immunopurified membranes for 30 min at 30°C in KB containing 10  $\mu$ Ci of [ $\gamma$ -<sup>32</sup>P]ATP and 0.1 mM ATP. The reaction was quenched by addition of 4 mM ATP (final concentration). Membranes were collected with a magnet and the remaining membrane fragments centrifuged at 100,000 rpm for 20 min in a TLA-100.2 rotor (Beckman Coulter, Fullerton, CA). Triton X-100 (1% final concentration) was added to the supernatants. ERK-1, p38<sup>MAPK</sup>, and JNK-1 were then immunoprecipitated, and their phosphorylation state was analyzed by radioautography after SDS-PAGE separation. In parallel, kinase activities were measured as described above. Alternatively, 30  $\mu$ g of immunopurified ER membranes prepared from Nck $^{+/+}$  MEFs, Nck $^{-/-}$  MEFs or FR3T3 cells transfected or not with either pcDNA3, pcDNA3/IRE1 $\alpha$ .Nck-1, or pcDNA3/Trap $\alpha$ .Nck-1 and treated or not with 10 mM Azc for 30 min to 2 h were incubated in the absence or presence of 1-5  $\mu$ g of recombinant Nck-1(3SH3)wt followed by incubation with either RLC or Nck-immunodepleted RLC for 30 min at 30°C in HB without BSA [HB (-BSA)]. Membranes and corresponding supernatants were separated using a magnet, resolved by SDS-PAGE and analyzed by immunoblot by using anti-CNX, anti-Nck, anti-ERK-1, and anti-phospho-ERK antibodies. To estimate the kinases activated specifically by the purified ER membranes, densitometric values used for the ratios of phospho-ERK-1 to ERK-1, phospho-JNK-1 to JNK-1, and phospho-p38<sup>MAPK</sup> to p38<sup>MAPK</sup> were normalized to the relative amount of CNX in each fraction.

### Association of Nck-1 with CNX-enriched Microsomes

CNX-enriched microsomes were prepared from Nck $^{-/-}$  MEFs treated for 30 min with 10 mM Azc as described above and incubated with or without 1, 2.5, or 5  $\mu$ g of recombinant Nck-1-3SH3 wt for 1 h at 4°C in HB (-BSA). Alternatively, clarified lysate from untreated Nck $^{-/-}$  MEFs was incubated successively with anti-CNX (C3+C4) antibodies and protein A-magnetic

beads as described for the immuno-isolation of the ER-enriched compartment. The beads were then incubated for 1 h at 4°C, in the presence of 5 µg of recombinant Nck-1(3SH3) wt. After separation from magnetic beads, supernatants were mixed with an equal volume of 2× Laemmli sample buffer, whereas magnetic beads were washed five times with HB (-BSA) before being mixed with Laemmli sample buffer. The amount of free or bead-associated Nck-1 and CNX was assessed by immunoblotting by using either anti-Nck or anti-CNX antibodies.

### Immunodepletion

One milligram of RLC was incubated with either anti-Nck or anti-Shc antibodies for 3 h at 4°C. A second round of immunodepletion was performed for an additional 3 h at 4°C followed by incubation with protein G-Sepharose beads for 45 min at 4°C. Beads were centrifuged for 30 s at room temperature, washed three times, and finally mixed with an equal volume of 2× Laemmli sample buffer, whereas the resulting supernatant was either mixed with an equal volume of 2× Laemmli sample buffer or used, as described above, for the cell-free SAPK/MAPK pathways activation assay.

### GST Pull-Down

BL21 bacteria expressing either GST, GST-IRE1α, GST-IRE1β, Nck-1 SH3-1-GST, Nck-1 SH3-2-GST, or Nck-1 SH3-3-GST were sonicated 3 × 30 s on ice and lysed with 20 mM Tris-HCl, pH 8.0, 150 mM NaCl, 1% TX-100, 1 mM NaF, 1 mM Na<sub>3</sub>VO<sub>4</sub>, 1 mM PMSF, 10 µg/ml leupeptin, and 10 µg/ml aprotinin for 30 min on ice. After 30-min centrifugation at 4°C, fusion proteins were purified with glutathione-Sepharose beads. Nck-1 SH3-1-GST, Nck-1 SH3-2-GST, and Nck-1 SH3-3-GST were digested with thrombin (Amersham Biosciences, Piscataway, NJ) for 3 h at room temperature according to the manufacturer's instructions. The resulting product was depleted of both thrombin and GST by sequential incubation with benzamide-Sepharose and glutathione-Sepharose beads, respectively. The resulting supernatant was then incubated with either GST-hIRE1α or GST-hIRE1β bound to glutathione-Sepharose beads for 2 h at 4°C in phosphate-buffered saline (PBS). Beads were collected, washed three times with PBS, and resuspended in Laemmli sample buffer before immunoblot analysis by using anti-GST and anti-Nck antibodies.

### Subcellular Localization and Immunofluorescence

FR3T3 cells grown in 24-well plates (1.5 × 10<sup>5</sup> cells/well) or in 15-cm dishes (8 × 10<sup>6</sup> cells/dish) were transiently transfected with either pcDNA3, pcDNA3/IRE1α-Nck-1, or pcDNA3/Trapα-Nck-1 (1 µg for the 24-well plates; 15 µg for the 15-cm dishes). Forty-eight h posttransfection, cells grown on the 15-cm dishes were washed with cold PBS and lysed in HB (-BSA), homogenized 10 times by using a 25<sup>3/8</sup> gauge syringe. Lysates were precleared and centrifuged at 100,000 rpm, 30 min at 4°C in a Beckman TLA-100.2 rotor. Proteins present in the resulting supernatant were trichloroacetic acid (TCA) precipitated, washed with 70% acetone, and mixed with Laemmli sample buffer, whereas the corresponding pellet was mixed with Laemmli sample buffer. Samples were resolved on SDS-PAGE and analyzed by immunoblot by using anti-Nck or anti-Myc antibodies. Alternatively, cells grown on 24-well plates were fixed with 3.7% formaldehyde for 10 min, permeabilized with 0.1% Triton-X 100 for 5 min, incubated with anti-myc and anti-BiP antibodies for 1 h at room temperature followed by incubation with anti-mouse TRITC and anti-rabbit FITC antibodies. The immunolocalization of myc-tagged IRE1α-Nck-1 and Trapα-Nck-1 as well as that of BiP was assessed by fluorescence microscopy by using a 63× 1.4 oil immersion objective (Carl Zeiss, Thornwood, NY), recorded with a digital camera (DVC, Austin, TX), and analyzed with Northern Eclipse software (Empix Imaging, Mississauga, ON, Canada).

### Semiquantitative Reverse Transcription-Polymerase Chain Reaction (RT-PCR) Analysis

Nck<sup>+/+</sup> and Nck<sup>-/-</sup> MEFs were grown in Dulbecco's modified Eagle's medium (DMEM) containing 10% fetal bovine serum (FBS) in the absence or presence of 10 mM Azc for 30 min to 2 h, and lysed in TRIzol (Invitrogen) for total RNA isolation. RNA was reverse transcribed to cDNA by using random hexamers and the ThermoScript RT-PCR system (Invitrogen). Ten percent of the cDNA synthesis reaction was submitted to semiquantitative PCR analysis for BiP, CHOP, XBP-1, and GAPDH expression by using *Taq*DNA polymerase (Fermentas, Burlington, ON, Canada). The following oligonucleotides were used: 5'-GGGAAAGAAGGTTACCCATGC and 5'-CGAGTAGATCCAC-CAACC AGAG for BiP; 5'-CCCTGCCTTACCTTGG and 5'-CCGCTCGT-TCTCTGCTC for CHOP; 5'-AACTCCAGCTAGAAAATCAGC and 5'-CCATGGGAAGATGTTCTGGG for XBP-1; 5'-ACCACCTGGAGAAGG-CTGG and 5'-CTCAGGTAGCCAGGATGC for GAPDH. PCR products in their linear range were analyzed on agarose gels.

### Cell Viability and Apoptosis Assays

Nck<sup>+/+</sup> and Nck<sup>-/-</sup> MEFs were plated on six-well plates at a density of 2 × 10<sup>5</sup> cells/well, and grown in DMEM + 10% FBS for 24 h. Cells were then

incubated in the absence or presence of 10 mM Azc. At the indicated times, cells were washed once with cold PBS, trypsinized, and counted. Apoptosis was assessed as follows: cells (4 × 10<sup>5</sup> cells/well in six-well plates) were grown for 16 h, followed by a 2- to 4-h incubation with or without 10 mM Azc. Cells were then stained with annexin V and propidium iodide (PI) by using an annexin V-FITC apoptosis detection kit I (BD Pharmingen, San Diego, CA) as recommended by the manufacturer. Annexin V-positive cells were analyzed by flow cytometry (BD Biosciences, San Jose, CA).

## RESULTS

### ER Stress-mediated MAPK/SAPK Activation Is Partially Dependent on IRE1α

Azc and Tun are two potent activators of ER stress (Barbosa-Tessmann *et al.*, 1999; Shen *et al.*, 2001). A 10-min treatment with Tun triggered mostly the activation of JNK-1 and p38<sup>MAPK</sup> in both FR3T3 cells and IRE1α<sup>+/+</sup> MEFs (black bars, Figure 1, A and B, middle and right), whereas this activation was significantly lower in IRE1α<sup>-/-</sup> MEFs (Figure 1B, middle and right). Azc treatment promoted the activation of ERK-1, (3.2-fold and 2.4-fold, respectively, grey bars, Figure 1, A and B, left), p38<sup>MAPK</sup> (2.2-fold and 2.4-fold, respectively, Figure 1, A and B, right), and JNK-1 (2.7-fold and 1.8-fold respectively, Figure 1, A and B, middle) in both FR3T3 cells and IRE1α<sup>+/+</sup> MEFs. However, Azc-induced ERK-1 activation in IRE1α<sup>-/-</sup> MEFs was completely abolished while p38<sup>MAPK</sup> and JNK-1 activation were significantly reduced (Figure 1, A and B). Sustained Azc and Tun treatments maintained elevated kinase activity levels (unpublished data). These results demonstrate the involvement of IRE1α in Azc-induced ERK-1, p38<sup>MAPK</sup>, and JNK-1 activation.

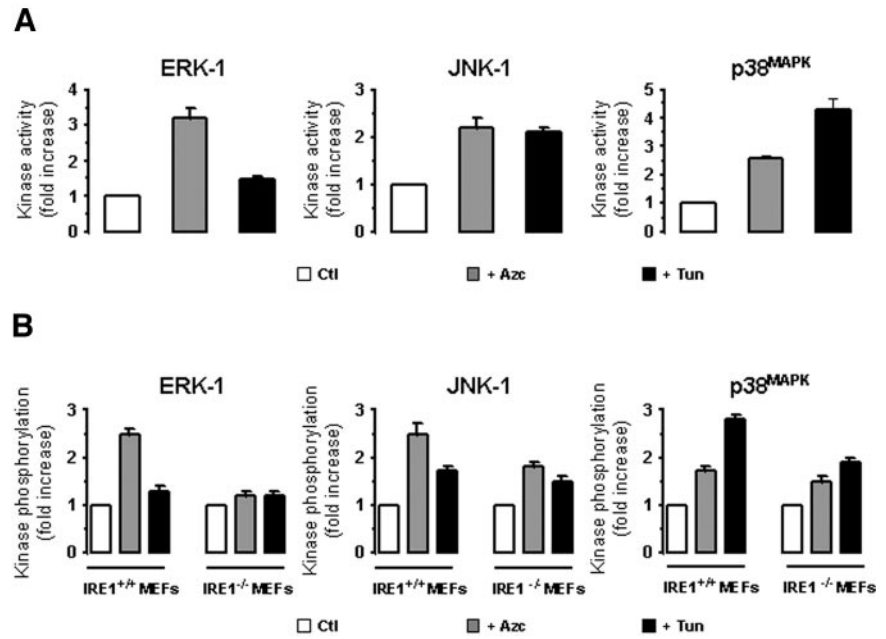
### Immuno-isolation and Characterization of ER from FR3T3 Cells

To dissect the molecular events leading to ER stress-mediated ERK-1 activation, we examined the activation of the MAPK/SAPK pathways in a cell-free system by using isolated ER membranes from FR3T3 cells treated or not with misfolding agent. CNX, an ER resident transmembrane protein that displays a cytosolic carboxy-terminal region (Ellgaard and Heleinus, 2003; Schrag *et al.*, 2003) was used as an antigen to immuno-isolate the compartment where it segregates. Similar approaches have been shown previously to successfully immuno-isolate membranes highly enriched in ER, endosomes, phagosomes or Golgi (Gruenberg and Howell, 1985; Gruenberg and Howell, 1986; Luers *et al.*, 1998) with the exception that here our method used anti-CNX antibodies as the membrane trap. Comparison of the protein composition of our immuno-purified ER membrane fraction to PNS by immunoblot analysis showed a ninefold-enriched CNX/ER fraction containing some mitochondria (Tom 20) but no Golgi or plasma membrane as shown with MG-160 and epidermal growth factor receptor (EGFR) markers, respectively (Figure 2A). Finally, electron microscopy revealed ribosome-containing ER membranes associated with ~20% of the magnetic beads and some mitochondria tightly apposed to ER membranes (Figure 2B). Control beads coupled to nonimmune serum revealed no associated membranes (unpublished data).

### Cell-free Reconstitution of ER Stress-mediated Activation of the MAPK/SAPK Pathways

To establish whether the MAPK/SAPK pathways could be activated using CNX-enriched membranes, we developed a cell-free assay by using ER immuno-isolated from FR3T3 cells pretreated or not with either Azc, Tun, or NaAs for 10 min. Membranes (100 µg) were incubated with RLC (3 mg of protein) for 30 min at 30°C supplemented or not with [ $\gamma$ -<sup>32</sup>P]ATP. The phosphorylation of cytosolic ERK-1, JNK-1,

**Figure 1.** Effect of Azc and Tun on MAPK/SAPK activation. ERK-1, JNK-1 or p38<sup>MAPK</sup> activities/phosphorylation states were analyzed in FR3T3 cells, IRE1 $\alpha^{+/+}$ , or IRE1 $\alpha^{-/-}$  MEFs after 10-min treatment with 10 mM Azc or 10  $\mu$ g/ml Tun. (A) JNK-1, p38<sup>MAPK</sup>, and ERK-1 were immunoprecipitated from clarified lysates obtained from FR3T3 cells, treated or not and immunoprecipitates were subjected to in vitro kinase assays with the following specific substrates: GST-Jun, GST-ATF2, and MBP respectively (n = 3, value  $\pm$  SD). (B) MEF lysates were directly immunoblotted either with anti-phospho-ERK, anti-phospho-JNK-1 or anti-phospho-p38<sup>MAPK</sup> antibodies. Immunoblots were quantified by scanning densitometry (n = 2). JNK-1, p38<sup>MAPK</sup>, and ERK-1 activation are reported in A and B, respectively, as fold increase in either activity (for FR3T3 samples) or phosphorylation (for MEF samples) over control.



and p38<sup>MAPK</sup> was assessed by radioautography (Figure 2C), and the corresponding kinase activity was measured by in vitro phosphorylation of specific substrates (Figure 2D) as described under *Materials and Methods*. The results showed that ERK-1, JNK-1, and p38<sup>MAPK</sup> activation profiles in microsomes immuno-isolated from Azc- or Tun-treated cells (Figure 2, C and D) were similar to those obtained in vivo (Figure 1). Therefore, these data demonstrate a specific role for the ER membrane in the activation of cytosolic MAPK/SAPK upon treatment of cells with ER stressors. As a negative control, NaAs did not affect any ER signaling pathways as reported previously (Brostrom *et al.*, 1996; Mengesdorf *et al.*, 2002).

Together, these results indicate that upon Azc or Tun treatment, the ER per se was able to activate signaling cascades leading to the activation of ERK-1, JNK-1, and p38<sup>MAPK</sup>. To rule out the possibility that the above-mentioned results were due to ER fractions contaminated by plasma membrane, a plasma membrane fraction was isolated using wheat germ agglutinin (WGA)-coated magnetic beads. These fractions showed a sevenfold enrichment of EGFR in the WGA-purified membrane compared with the ER marker Ribophorin I, which was undetectable (unpublished data). We also tested ERK-1, p38<sup>MAPK</sup>, and JNK-1 phosphorylation levels induced by plasma membrane fraction purified from cells treated or not with 10 mM Azc for 10 min to 2 h, and no significant phosphorylation was detected for these kinases (unpublished data).

### Role of ER-associated Adaptor Proteins in Mediating ER Stress Signaling

Because adaptor proteins play a major role in the extracellular activation of MAP kinases, we investigated whether such scaffolding proteins could be implicated in related signaling pathways emerging from the ER. Consistent with this idea, Shc localizes at the ER membrane (Lotti *et al.*, 1996) and TRAF-2 is recruited by IRE1 upon ER stress to mediate JNK-1 activation (Urano *et al.*, 2000a). A screen for known adaptor proteins involved in signal transduction revealed, as expected, a significant amount of ER-associated Shc, and

surprisingly, led to the identification of the SH2/SH3 containing adaptor protein Nck in the same immuno-isolated membranes as compared with the PNS fraction (Figure 3A). In contrast, the adaptors Grb-2 and Crk were detected only in the PNS (Figure 3A). To test whether Shc or Nck could participate in the activation of the MAPK/SAPK pathways from stressed ER, RLC was immunodepleted either of Shc or Nck by using their respective antibodies (Figure 3B). These RLCs were then added to ER membranes immuno-isolated from Azc- or Tun-treated FR3T3 cells in the presence or not of the following recombinant proteins: 3SH3 domains of Nck-1 or the SH2 domain of Shc (Figure 3, C and D).

Interestingly, after the reconstitution of the kinase pathway by using Nck-immunodepleted RLCs, the major effect was only observed on ERK-1 activation (Figure 3C; Supplementary Data, Table 1). Indeed, nonimmunodepleted cytosols triggered a 2.9-fold induction of ERK-1 activity upon Azc treatment, whereas addition of cytosol immunodepleted of Nck led to a reduced ERK-1 activation (1.4-fold increase over ctl) (black bars, Figure 3C). Most importantly, the reduced ERK-1 activation observed in Nck-immunodepleted cytosols was still significantly higher than the activation obtained with control cytosol. The observed decrease could be reversed by adding back wild-type recombinant Nck-1(3SH3) protein (3.6-fold increase over ctl, Figure 3C) but not by the recombinant Nck-1(3SH3) protein containing nonfunctional mutations in its 3SH3 domains (Supplementary Data, Table 1). In addition, Nck immunodepletion showed an effect on the maintenance of ERK-1 basal activity upon Tun treatment (10-fold decrease over ctl, Figure 3C), which was also dependent on the integrity of the 3SH3 domains of Nck-1. Together, these results indicated a role for Nck-1 SH3 domains in mediating ER activation of the ERK pathway during Azc-mediated stress.

To assess the specificity of the effects observed with Nck, similar experiments were performed in Shc-immunodepleted RLC. No significant change in kinase activities was detected (Figure 3D; Supplementary Data, Table 1). However, the add-back experiment with an excess of wt Shc-SH2 domain notably decreased Azc-induced ERK-1 activity,

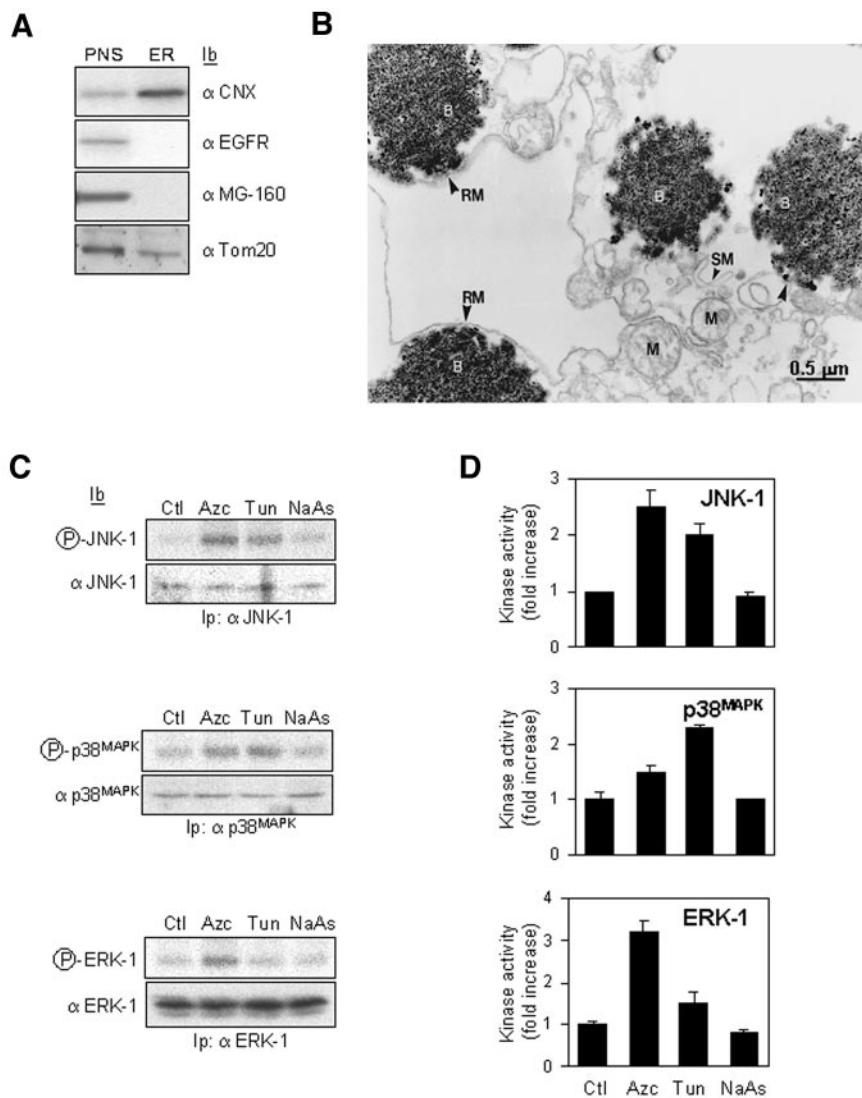


**Figure 2.** ER immuno-isolation and in vitro reconstitution of ER stress-activated signaling pathways. (A) Biochemical analysis of the immunopurified membranes by using CNX as the ER membrane trap. In each lane, total protein corresponding either to 10% of the PNS or to the total immunopurified membranes (ER) were immunoblotted with anti-CNXX, anti-EGF receptor (plasma membrane marker), anti-MG-160 (Golgi marker), or anti-Tom20 (mitochondrial marker). (B) Morphological analysis of the immunopurified CNX compartment. Immunopurified membranes were treated as described under *Materials and Methods*. Rough membranes (RM), smooth membranes (SM), mitochondria (M), and magnetic beads (B). Bar, 0.5 μm. (C) Cells were treated with 10 mM Azc, 10 μg/ml Tun, or 50 μM NaAs for 10 min. CNX-enriched membranes were immunopurified as described under *Materials and Methods*. Each sample (~1 mg of protein) was divided in three equal fractions (~300 μg of protein each) and incubated with 3 mg of cytosol purified from rat liver. The phosphorylation level of ERK-1, JNK-1, or p38<sup>MAPK</sup> is shown (top gels); the amount of kinase was assessed by immunoblotting (bottom blots). (D) For each kinase, the ER stress-induced activity was quantified by the in vitro phosphorylation of GST-Jun, GST-ATF2 or MBP by immunoprecipitated JNK-1, p38<sup>MAPK</sup>, or ERK-1 respectively (n = 3, value ± SD).

whereas addition of an excess of nonfunctional Shc-SH2 domain had no effect on ERK-1 activation (Figure 3D; Supplementary Data, Table 1). This result indicates that an excess of Shc-SH2 domain negatively regulates Azc-induced ERK-1 activation.

#### ***Nck Associates with the ER Membrane and Binds to IRE1 Proteins***

Based on the above-mentioned results, we hypothesized that Nck and IRE1 proteins may be involved in the same signaling process, leading to ERK-1 activation during Azc-mediated stress. To further validate the presence of a pool of Nck associated with the ER membrane, subcellular compartments (rough ER, RER; smooth ER, SER; ER-Golgi intermediate compartment, ERGIC and Golgi) were isolated from rat liver by centrifugation of liver homogenate on discontinuous sucrose gradients as described previously (Nelson *et al.*, 1998; Lavoie *et al.*, 2000; Bell *et al.*, 2001). The presence of Nck, the ER resident molecular chaperone BiP, and IRE1 $\alpha$  was assessed by immunoblotting of these fractions with their respective antibodies. IRE1 $\alpha$  and BiP were detected mainly in RER, SER, and ERGIC, whereas Nck was found in all membrane fractions (Figure 4), thus confirming the re-

sults obtained previously with the immuno-purified ER membranes.

Our results show that Nck is associated with ER membranes (Figure 3A), localizes in the same compartments as IRE1 (Figure 4), and modulates in vitro the ER stress-induced ERK-1 activation through its SH3 domains (Figure 3C). In addition, we showed that the ER stress-mediated activation of ERK-1 was dependent on IRE1 proteins (Figure 1). Therefore, we postulated that IRE1 and Nck may be part of the same molecular complex interacting either biologically or physically. Analysis of the IRE1 protein sequence identified the presence of three canonical PxxP motifs within IRE1 $\alpha$  carboxy-terminal region and one motif within IRE1 $\beta$  carboxy-terminal region. Because these motifs are known to bind SH3 domains, we therefore tested whether the SH3 domains of Nck-1 (Figure 5A) could bind to the cytosolic domains of IRE1 $\alpha$  and IRE1 $\beta$ . Interestingly, IRE1 $\alpha$  associated mainly with SH3-1, whereas IRE1 $\beta$  preferentially interacted with SH3-3 (Figure 5B). These results showed in vitro, a direct interaction between IRE1 and Nck-1 SH3 domains. To further demonstrate that Nck-1 associated with IRE1 in the ER, rat liver SER, RER, and Golgi microsomes were solubilized and the clarified lysates were immunoprecipi-

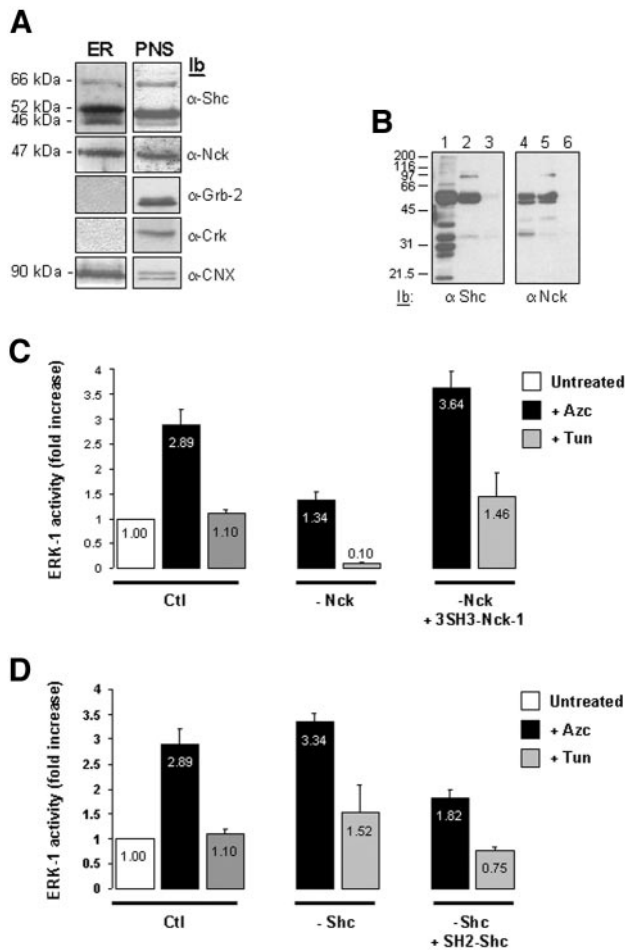


**Figure 3.** Immunodepletion of cytosolic Nck alters the ER stress-mediated activation of ERK-1. (A) Immunoblotting of the ER immuno-isolated from FR3T3 cells with anti-Shc, anti-Nck, anti-Grb2, anti-Crk, and anti-CNX antibodies. A representative experiment is shown ( $n = 4$ ). The same amount of total proteins corresponding either to total immuno-isolated ER membranes (ER) or 10% of the PNS were immunoblotted with anti-Shc, anti-Nck, anti-Grb-2, anti-Crk, and anti-CNX antibodies. (B) Shc and Nck immunodepletion from cytosol. Lanes 1 and 2 and 4 and 5, subsequent immunoprecipitations of the total cytosol with anti-Shc or anti-Nck antibodies, followed by an immunoblot with respective antibodies. Lanes 3 and 6, Shc and Nck immunoblots of Shc- or Nck-immunodepleted cytosol. (C) ER microsomes immuno-isolated from nontreated, 10 mM Azc, or 10  $\mu$ g/ml Tun treated cells were incubated with control RLC (Ctl), or RLC that had been previously Nck-immunodepleted (-Nck) either in the presence or absence of 10  $\mu$ g of recombinant 3SH3-Nck-1 wt. ERK-1 activity is shown. Results are presented as fold increase over control (Azc, black bars; Tun, gray bars;  $n = 2$ , value  $\pm 0.5$  variation). Values in the graph bars indicate the relative ERK-1 activity. (D) Same experiment as in C except that ER microsomes were incubated with control RLC (Ctl), or RLC that had been previously Shc-immunodepleted (-Shc) either in the presence or absence of 10  $\mu$ g of recombinant SH2-Shc wt. ERK-1 activity is shown. Results are presented as fold increase over control (Azc, black bars; Tun, gray bars;  $n = 2$ , value  $\pm 0.5$  variation). Values in the graph bars indicate the relative ERK-1 activity.

tated with anti-Nck antibodies. Immunoprecipitates were then immunoblotted with anti-IRE1 $\alpha$  antibodies. IRE1 $\alpha$  was detected in both SER and RER lysates but not in Golgi lysates (Figure 5C). This was not due to nonspecific binding of IRE1 $\alpha$  to the protein A-Sepharose beads because IRE1 $\alpha$

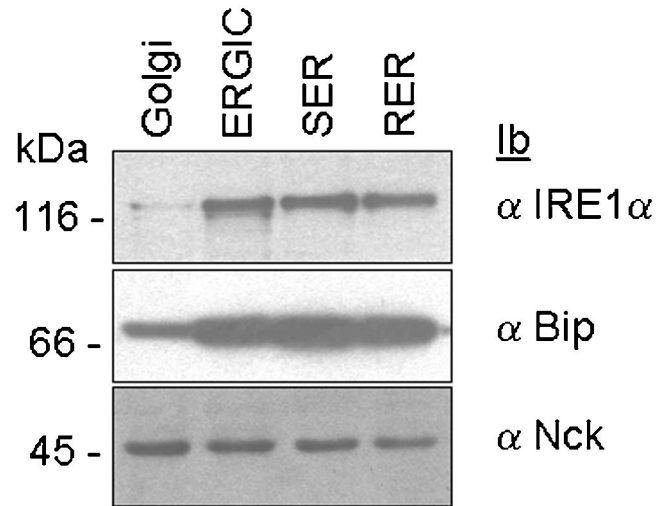


**Figure 4.** Distribution of BiP, Nck, and IRE1 $\alpha$  in purified membrane fractions. Rough ER (RER), smooth ER (SER), ER-Golgi intermediate compartment (ERGIC) and Golgi were fractionated and purified from rat livers as reported previously (Lavoie *et al.*, 2000). Each fraction was then immunoblotted with anti-BiP (middle), anti-Nck (bottom), or anti-IRE1 $\alpha$  (top) antibodies ( $n = 2$ ).

could not be detected in Shc immunoprecipitates (Figure 5C). These results confirmed the specificity of the IRE1 $\alpha$  and Nck interaction in the ER compartment.

#### ER-associated Nck-1 Regulates ER Stress Signaling In Vitro

Based on the observation that Nck was involved in ER stress-induced ERK-1 activation in vitro, we investigated whether the pool of Nck bound to ER membranes could be critical for ER stress-induced ERK-1 activity. To test this hypothesis, we reconstituted the activation of ERK-1 in vitro by using immuno-isolated ER membranes from MEFs lacking both isoforms of Nck, Nck-1 and Nck-2 (Nck $^{-/-}$ ) and that had been previously incubated in the absence or the presence of 10 mM Azc for 30 min. The immuno-isolated ER membranes from these cells were then incubated with various amounts of recombinant Nck-1(3SH3) to assess the association of Nck-1 with the ER membranes. Recombinant Nck-1(3SH3) added exogenously was able to bind to ER membranes isolated from untreated Nck $^{-/-}$  MEFs (Figure 6A, left), consistent with the constitutive association of Nck with the ER observed in FR3T3 cells (Figure 3A). Indeed, this association was not due to artifactual adsorption of recombinant Nck-1(3SH3) onto magnetic beads, because recombinant Nck-1(3SH3) did not associate with the beads in the absence of membranous structures (Figure 6A, right). Surprisingly, as shown in Figure 6A (left panel), Azc treatment led to reduced association of recombinant Nck-1(3SH3) to ER microsomes. Indeed, both the affinity and the binding capacity of ER membranes for Nck were reduced upon Azc treatment, suggesting a dissociation of ER-membrane bound Nck during stress.

To functionally assess the signaling potential of ER immuno-isolated from Nck $^{+/+}$  or Nck $^{-/-}$  MEFs, both cell lines were treated with 10 mM Azc for 30 min. ER was then immuno-isolated from these cells and assayed for ERK-1 activation in vitro. Interestingly, ER purified from untreated Nck $^{-/-}$  MEFs induced ERK-1 phosphorylation (1.4-fold higher than ER purified from wild-type cells; Figure 6B). In

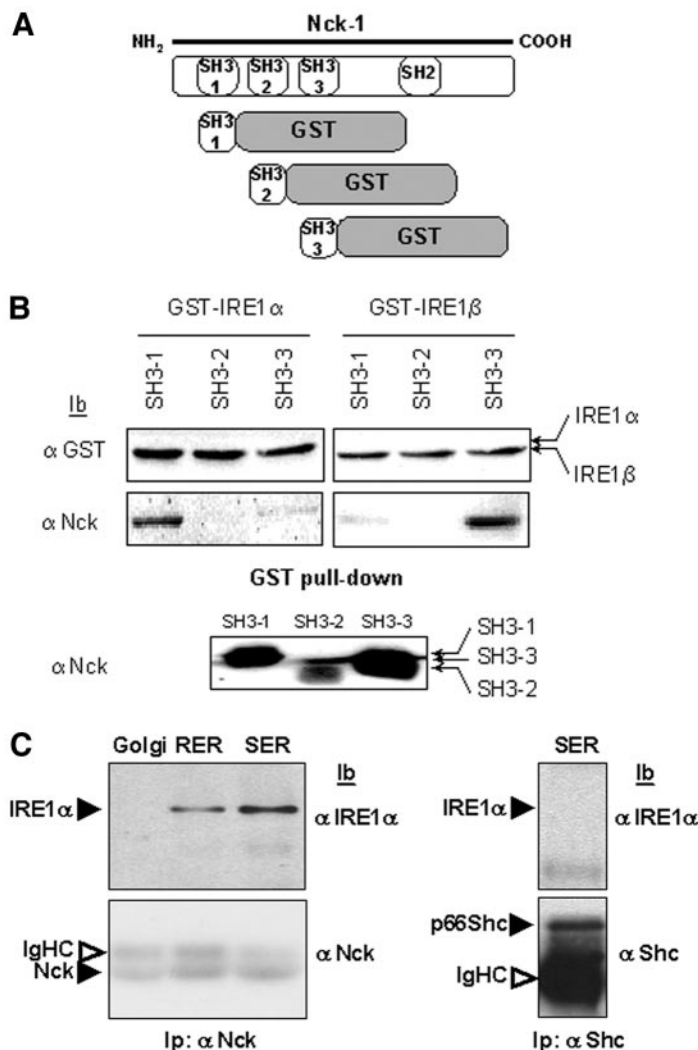


**Figure 5.** In vitro association of Nck-1 SH3 domains with IRE1 cytosolic domain. (A) Representative scheme of the chimera constructed for these studies. (B) Individual SH3 domains of Nck-1, Nck-1-SH3(1), Nck-1-SH3(2), and Nck-1-SH3(3), fused to GST were cleaved with thrombin, GST and thrombin were depleted and the products were pulled down with GST-IRE1 $\alpha$  or GST-IRE1 $\beta$  bound to glutathione-Sepharose beads. GST-associated proteins were immunoblotted with either anti-GST (top) or anti-Nck antibodies (middle). The input of Nck-1-SH3(1), Nck-1-SH3(2), and Nck-1-SH3(3) domains was blotted with anti-Nck antibodies (bottom). (C) Rat liver Golgi or ER microsomes were solubilized, and clarified lysates (1 mg) were immunoprecipitated with anti-Nck antibodies. Immunoprecipitates were resolved by SDS-PAGE, transferred onto nitrocellulose membrane, and immunoblotted with either anti-IRE1 $\alpha$  or anti-Nck antibodies (n = 3).

addition, ER purified from both Nck<sup>+/+</sup> and Nck<sup>-/-</sup> MEFs treated with Azc induced ERK-1 phosphorylation (1.4- and 1.5-fold over untreated ER, respectively; Figure 6B). These results suggest that ER membranes purified from Nck<sup>+/+</sup> and Nck<sup>-/-</sup> MEFs treated with Azc are able to elicit ERK-1 phosphorylation as described for ER purified from FR3T3 cells. Moreover, basal ERK-1 activating potential in ER membranes purified from Nck<sup>-/-</sup> MEFs is higher than that from Nck<sup>+/+</sup> MEFs.

To test whether the association of Nck-1 with ER membranes was required for ERK-1 activation upon stress, ER membranes purified from either Azc treated or untreated Nck<sup>-/-</sup> MEFs were incubated with Nck-depleted RLC in the presence or absence of recombinant wild-type Nck-1(3SH3). Immunoblot analysis of CNX and Nck-1 for the membrane fractions was carried out (unpublished data), and levels of ERK-1 phosphorylation were assessed in the cytosol (Figure 6C). Regardless a stress was applied or not, immunodepletion of Nck from the RLC did not affect ERK-1 phosphorylation as compared with nonimmunodepleted RLC (Figure 6C, lanes 2, 3, 7, and 8). In addition, preincubation of recombinant Nck-1(3SH3) with ER membranes purified from nonstressed cells before incubation with immunodepleted RLC showed no change in the level of ERK-1 phosphorylation (Figure 6C, lanes 3–5). However, binding of

recombinant Nck-1(3SH3) to ER membranes immuno-isolated from Azc-stressed cells before incubation with Nck-depleted RLC led to a significant increase of ERK-1 phosphorylation (1.7- to 2-fold increase; Figure 6C, lanes 8–10). When ERK-1 was immunoprecipitated from the corresponding cytosolic fractions (immunodepleted or not of Nck and incubated with recombinant Nck-1(3SH3)-bound ER membranes immuno-isolated from nonstressed and Azc-stressed cells) and used for in vitro phosphorylation of MBP, similar ERK-1 activity profiles were obtained (unpublished data). These data suggest that Nck is required for ER stress-mediated ERK-1 activation in vitro.

#### Dissociation of Nck from the ER Membrane Is a Prerequisite for ER Stress-induced ERK-1 Activation

Based on the above-mentioned observations, we investigated whether the constitutive expression of Nck-1 at the ER membrane had an impact on ERK-1 activation in ER membranes purified from Azc-stressed cells. The luminal and transmembrane domains of IRE1 $\alpha$  and Trap $\alpha$ , an ER resident transmembrane protein involved in translocation (Fons *et al.*, 2003), were fused upstream of full-length Nck-1 (Figure 7A). In FR3T3 cells transiently transfected with these constructs, recombinant myc-tagged IRE1 $\alpha$ .Nck-1 and Trap $\alpha$ .Nck-1 localized, as expected, in

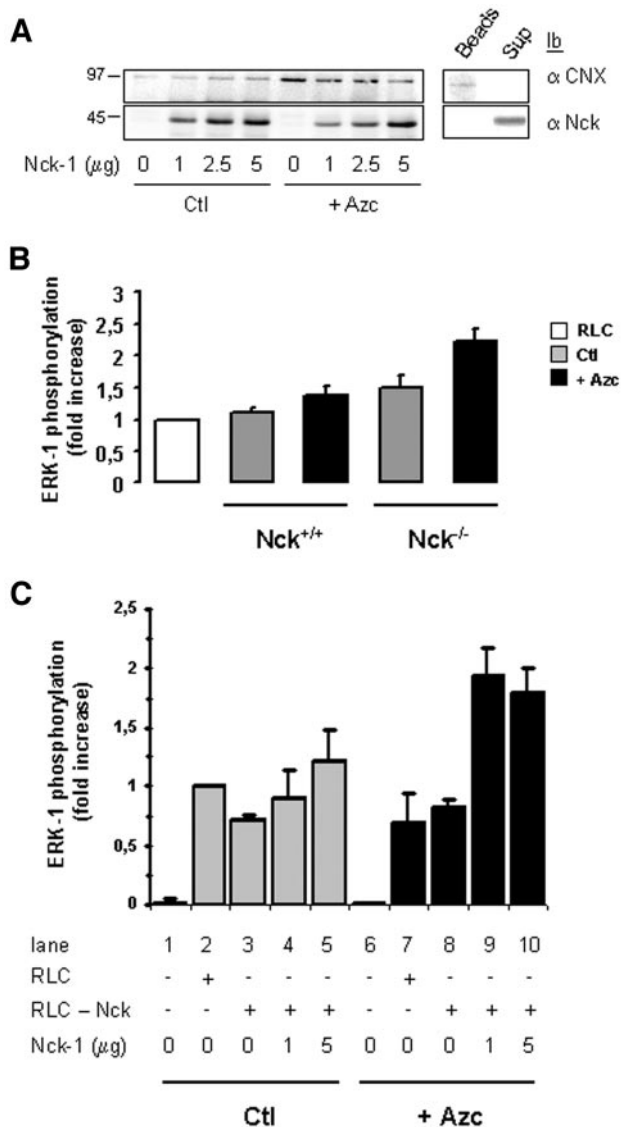


**Figure 6.** ER stress-mediated ERK-1 activation requires the association of Nck-1 with ER membranes. (A) ER immuno-isolated from  $Nck^{-/-}$  MEFs treated or not with 10 mM Azc for 30 min was divided into four equal fractions and incubated in the absence or presence of 1, 2.5, or 5  $\mu$ g of recombinant Nck-1(3SH3) wt. Magnetic beads were washed extensively and Nck-1 association to these membranes was assessed by immunoblotting by using anti-Nck (bottom left) and anti-CNX antibodies (top left). A representative immunoblot is shown ( $n = 4$ ). Clarified lysate from untreated  $Nck^{-/-}$  MEFs was incubated successively with anti-CNX antibodies and protein A-magnetic beads as described under *Materials and Methods* section for the immuno-isolation of ER enriched membranes, and the mixture was then incubated in the presence of 5  $\mu$ g of recombinant Nck-1(3SH3) wt. After separation with a magnet, the supernatant was collected and the magnetic beads were washed extensively. The association of CNX and Nck-1 with the beads (Beads) or their presence in the incubation medium (Sup) was assessed by immunoblotting by using anti-CNX (top right) and anti-Nck (bottom right) antibodies. (B) RLC was incubated in the absence (white bar) or in the presence of ER purified from  $Nck^{+/+}$  MEFs or  $Nck^{-/-}$  MEFs treated (black bars) or not (gray bars) with 10 mM Azc for 30 min. The phosphorylation state of ERK-1 was assessed as described under *Materials and Methods* section ( $n = 2$ , value  $\pm 0.5$  variation). (C) ER was purified from  $Nck^{-/-}$  MEFs treated as in A. Each sample ( $\sim 1$  mg of protein) was divided into five equal fractions and incubated in the absence of RLC (conditions

the membrane fractions but not in the soluble fractions as shown by immunoblot by using both anti-myc and anti-Nck antibodies (Figure 7B). Colocalization of IRE1 $\alpha$ .Nck-1 and Trap $\alpha$ .Nck-1 with BiP in an ER-like, perinuclear compartment was further confirmed by immunofluorescence microscopy by using anti-BiP and anti-myc antibodies (Figure 7C). To characterize the effect of IRE1 $\alpha$ .Nck-1 and Trap $\alpha$ .Nck-1 on ERK-1 activation by Azc-stressed microsomes, FR3T3 cells were transiently transfected with either pcDNA3 (Empty), pcDNA3/IRE1 $\alpha$ .Nck-1 (IRE1 $\alpha$ .Nck-1) or pcDNA3/Trap $\alpha$ .Nck-1 (Trap $\alpha$ .Nck-1). Forty-eight hours posttransfection, cells were incubated with Azc for 30 min to 2 h, and then ER membranes were isolated and further incubated in the presence of RLC. The membrane and soluble fractions were separated and immunoblot analysis of CNX in the membrane fractions and ERK-1 and phospho-ERK1/2 in the soluble fractions was performed. ER membranes isolated from cells transfected with the empty vector and incubated with RLC were able to promote a 1.3- and 1.8-fold increase in ERK-1 activation after 30 min and 2 h of Azc treatment, respectively (white bars, Figure 7D). Under the same conditions, ER membranes isolated from cells expressing IRE1 $\alpha$ .Nck-1 or Trap $\alpha$ .Nck-1 and treated or not with Azc were significantly less efficient in activating ERK-1 (gray bars and black bar, respectively, Figure 7D). Interestingly, when ERK-1 activation was assessed in whole cell lysates from FR3T3 cells transfected with either the empty vector, pcDNA3/IRE1 $\alpha$ .Nck-1, or pcDNA3/Trap $\alpha$ .Nck-1 and treated with Azc for 30 min to 2 h, ERK-1 phosphorylation profiles were similar to those observed in the *in vitro* assay performed in the presence of intact RLC but with a significant reduction of Azc-induced ERK-1 activation in cells expressing either IRE1 $\alpha$ .Nck-1 or Trap $\alpha$ .Nck-1, compared with mock-transfected cells (Figure 7E). These data strengthen our hypothesis according to which ER membrane-associated Nck negatively regulates ER stress signaling and that ER stress-mediated ERK-1 activation requires dissociation of Nck from the ER membrane.

#### *Nck-Null Cells Elicit Resistance to Azc-induced Apoptosis*

To investigate the role of endogenous Nck during the UPR, semiquantitative RT-PCR experiments were carried out using total RNA isolated from  $Nck^{+/+}$  and  $Nck^{-/-}$  MEFs treated with 10 mM Azc for 30 min to 2 h to assess the transcriptional profile of Bip, CHOP, XBP-1 and GAPDH mRNAs. In both cell lines, Azc treatment led to the same levels of BiP and CHOP mRNA up-regulation (2.5- and 3.5-fold, respectively, Figure 8A), whereas the splicing profiles of XBP-1 mRNA remained the same (Figure 8A). Because our above-mentioned data suggested a critical role for Nck-1 in the activation of ERK-1 upon Azc stress (Figures 3C, 6, and 7), we tested the effect of Nck gene deletion on the activation of ERK-1 after Azc stress. Interestingly, as observed *in vitro*, ERK-1 basal phosphorylation was higher in  $Nck^{-/-}$  than in  $Nck^{+/+}$  MEFs (Figure 8B). Treatment of

1 and 6), in the presence of RLC (2 and 7), in the presence of Nck-depleted RLC (conditions 3 and 8), or in the presence of 1  $\mu$ g (conditions 4 and 9) or 5  $\mu$ g (conditions 5 and 10) of recombinant Nck-1(3SH3) wt for 1h on ice before incubation with Nck-depleted RLC for 30 min at 30°C. Membrane and cytosolic fractions were separated with a magnet. Magnetic beads were washed extensively and immunoblotting was performed with anti-CNX and anti-Nck antibodies on the membrane fractions and with anti-ERK-1 and anti-phospho-ERK antibodies on the cytosolic fractions. Results are presented as fold increase of ERK-1 phosphorylation over ctl + RLC ( $n = 3$ , value  $\pm$  SD).

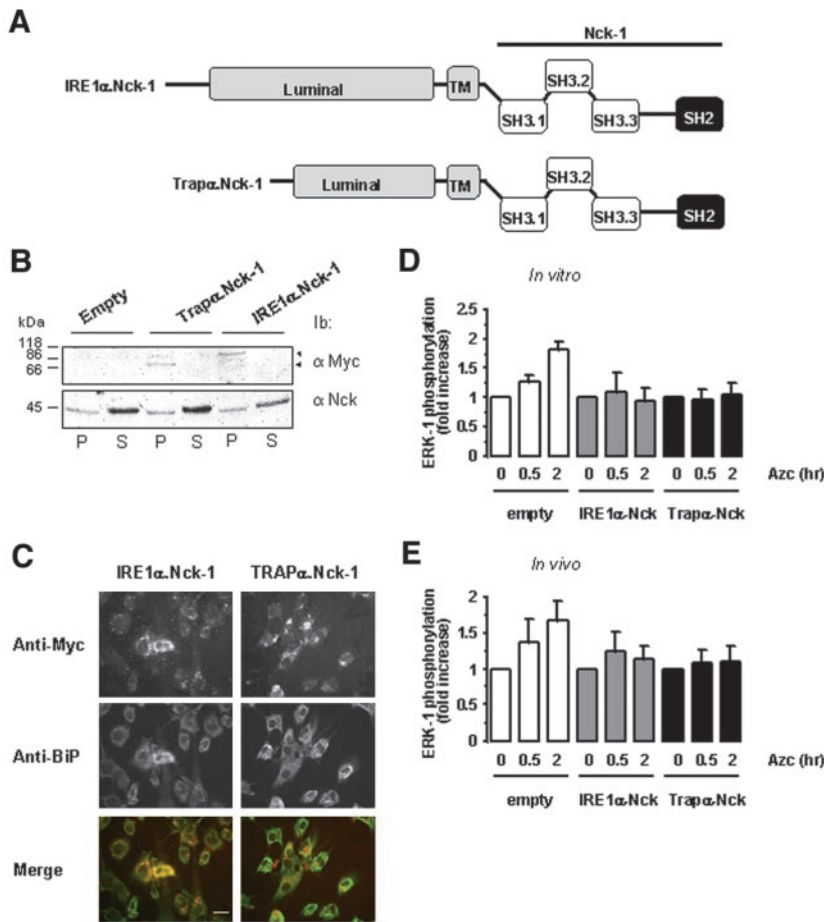


**Figure 7.** Forced localization of Nck-1 at the ER membrane affects ER stress-mediated ERK-1 activation. (A) Representative scheme of the fusion proteins IRE1 $\alpha$ .Nck-1 and Trap $\alpha$ .Nck-1 used. The luminal and transmembrane domains (gray) of IRE1 $\alpha$  or Trap $\alpha$  were fused to the wild-type full-length Nck-1. These constructs were myc-tagged at the C terminus. (B) FR3T3 cells were transfected with pcDNA3, pcDNA3/IRE $\alpha$ .Nck-1, or pcDNA3/Trap $\alpha$ .Nck-1, and expression of the respective recombinant protein was tested by immunoblot with anti-myc antibodies in the membrane fraction (P) and in the soluble fraction (S) (top blot). This was compared with the endogenous Nck content in both fractions by immunoblotting with anti-Nck antibodies (bottom blot). A representative immunoblot is shown (n = 3). (C) Immunofluorescence study of FR3T3 cells transfected with pcDNA3/IRE $\alpha$ .Nck-1 or pcDNA3/Trap $\alpha$ .Nck-1. Cells were immuno-stained with anti-myc antibodies (top) and anti-BiP antibodies as an ER marker (middle). Costaining was detected by merging of both pictures (bottom). A representative picture is shown (n = 3). Bar, 20  $\mu$ m. (D) *In vitro* reconstitution of ERK-1 activation in the presence of RLC was performed as described under *Materials and Methods*. These experiments were carried out using ER membranes purified from FR3T3 cells transfected with either pcDNA3 (empty) pcDNA3/IRE $\alpha$ .Nck-1 or pcDNA3/Trap $\alpha$ .Nck-1 and treated with 10 mM Azc for 0.5 and 2 h. (n = 2, value  $\pm$  0.5 variation). (E) ERK-1 phosphorylation in FR3T3 cells transiently transfected either with pcDNA3 (empty) pcDNA3/IRE $\alpha$ .Nck-1 or pcDNA3/Trap $\alpha$ .Nck-1 and treated with 10 mM Azc for 0.5 and 2 h (n = 2, value  $\pm$  0.5 variation). Lysates were directly immunoblotted with anti-phospho-ERK and anti-ERK-1 antibodies. Immunoblots were quantified by scanning densitometry (n = 2, value  $\pm$  0.5 variation).

Nck<sup>+/+</sup> MEFs with Azc for 30 min to 2 h led to a slight but significant increase in ERK-1 activation (1.6-fold increase, white bars, Figure 8B). Surprisingly, however, this activation was significantly higher in Nck<sup>-/-</sup> MEFs under the same conditions (2.1-fold increase, black bars, Figure 8B). Because the activation of ERK-1 promotes cell proliferation and survival (Wada and Penninger, 2004), we then tested whether the latter observation could reflect a difference in tolerance to Azc-induced ER stress between Nck<sup>+/+</sup> MEFs and Nck<sup>-/-</sup> MEFs. Indeed, we observed that Nck<sup>-/-</sup> MEFs were more tolerant to sustained Azc treatment than wild-type MEFs (Figure 8C). Under these conditions, the time required to obtain 50% lethality upon Azc exposure was 8 h for the Nck<sup>+/+</sup> MEFs and >12 h for the Nck<sup>-/-</sup> MEFs.

We next investigated whether the higher tolerance of the Nck-null cells to Azc exposure correlated with Azc-induced apoptotic levels. Nck<sup>+/+</sup> and Nck<sup>-/-</sup> cells either treated or not with Azc for 2 and 4 h, and then labeled with annexin V and PI, were analyzed by flow cytometry. Nck<sup>+/+</sup> cells showed a significant increase for late apoptotic and/or necrotic (PI-positive labeling and annexin V-positive labeling) cells at 2-h Azc treatment (1.3-fold increase, Figure 8D, top) and reached a 1.9-fold increase after 4-h treatment. However, Azc treatment did not significantly affect the populations of apoptotic Nck<sup>-/-</sup> cells under the same conditions as the wild-type (Figure 8D, bottom). These results confirm that during ER stress, cell survival correlates with elevated ERK-1 activation in the Nck-null cells and demonstrates a role for Nck in Azc-induced apoptosis.

## DISCUSSION

The concept of signaling from the ER has emerged in the past few years, and more recently interest has focused on ER stress proximal events such as IRE1- or ATF6-dependent signaling pathways (Hampton, 2000; Urano *et al.*, 2000a; Kaufman *et al.*, 2002; Zhang and Kaufman, 2004). However, most of the complex mechanisms regulating the ER proximal signaling events by which cell behavior and transcriptional responses are altered remain to be characterized. Here, we have used both *in vivo* and *in vitro* approaches to characterize the signaling intermediates involved in ER stress signaling responsible for the MAPK pathway activation.

### ER Stress Signals Are Transmitted through Adaptor Molecules

We established a cell-free assay based on the immuno-isolation of a CNX-enriched compartment to characterize the activation of the MAPK/SAPK pathways via the stress-induced ER. Based on previous reports indicating the involvement of the docking molecule TRAF-2 in ER stress signaling (Hampton, 2000; Urano *et al.*, 2000a; Kaufman *et al.*, 2002), we postulated that ER stress-mediated activation of the MAPK/SAPK pathways may involve other adaptor molecules known to participate in "conventional" signaling by cytokine receptors at the plasma membrane (Pawson and Saxton, 1999; Chang and Karin, 2001). Interestingly, in addition to Shc, which was previously reported to be ER associated (Lotti *et al.*, 1996), only Nck was detected in the

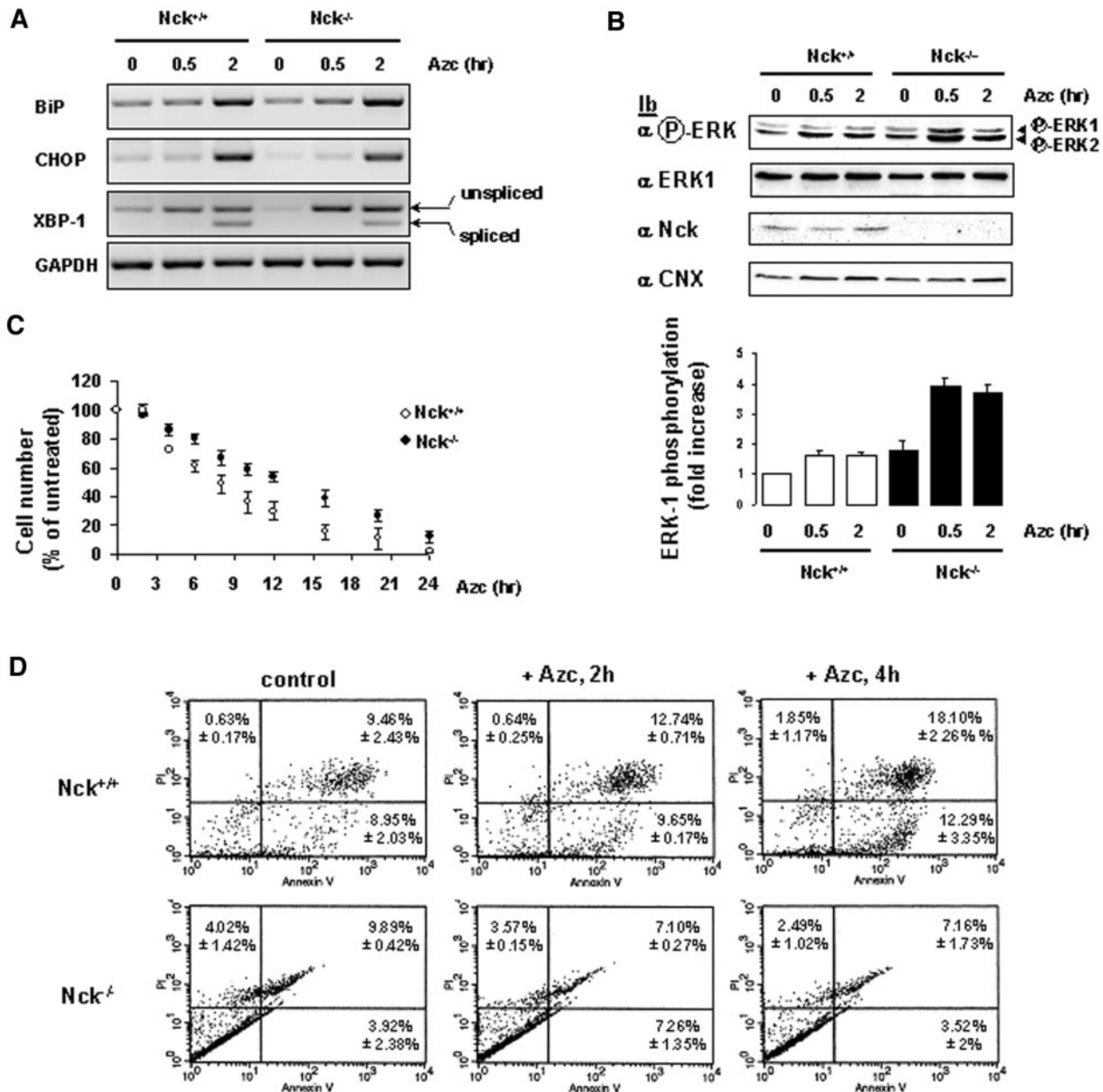


**Figure 8.** Nck mediates Azc-induced apoptosis. (A) RT-PCR analysis of Bip, CHOP, XBP-1, and GAPDH mRNA expression in Nck<sup>+/+</sup> and Nck<sup>-/-</sup> MEFs treated with 10 mM Azc for 0.5 to 2 h. A representative agarose gel of the RT-PCR assay is shown (n = 2). (B) ERK-1 phosphorylation was analyzed in Nck<sup>+/+</sup> and Nck<sup>-/-</sup> MEFs after treatment with 10 mM Azc for 0.5 and 2 h. MEFs lysates were directly immunoblotted either with anti-phospho-ERK, anti-ERK-1, anti-Nck, and anti-CNX antibodies. Immunoblots were quantified by scanning densitometry. A representative immunoblot is shown (n = 5, value ± SD). (C) Nck<sup>+/+</sup> and Nck<sup>-/-</sup> MEFs were treated with 10 mM Azc for 2 to 24 h. At each time point, the number of cells remaining after Azc treatment was compared with that of cells grown for the same time in Azc-free medium (n = 2, value ± 0.5 variation). (D) Nck<sup>+/+</sup> and Nck<sup>-/-</sup> MEFs were untreated (control) or treated with 10 mM Azc for 2 h (+Azc, 2 h) or 4 h (+Azc, 4 h) at which point apoptosis was determined by flow cytometry. A representative fluorescence-activated cell sorting analysis is shown (n = 2, value ± 0.5 variation).

immuno-isolated ER fraction. Together with the fact that Shc and Nck participate in the regulation of the MAPK/SAPK pathway from the plasma membrane (Buday, 1999), our observations suggest that they also may play a functional role in stress-induced ER signaling.

#### Nck Participates in ER Stress-induced ERK-1 Activation

To further characterize the involvement of Nck and Shc proteins in ER signaling, we carried out Nck or Shc immu-

nodepletion of the cytosol used in the in vitro kinase assay. The activation profiles of ERK-1, JNK-1, or p38<sup>MAPK</sup> obtained using Shc-immunodepleted cytosols were similar to those generated using normal cytosols. In contrast, the presence of Nck in the cytosol was required to promote ERK-1 activation by ER membranes purified from Azc-treated cells. Moreover, the "add-back" experiments suggested that at least the 3SH3 domains of Nck-1 were required for ERK-1 activation by ER membranes purified from Azc-stressed

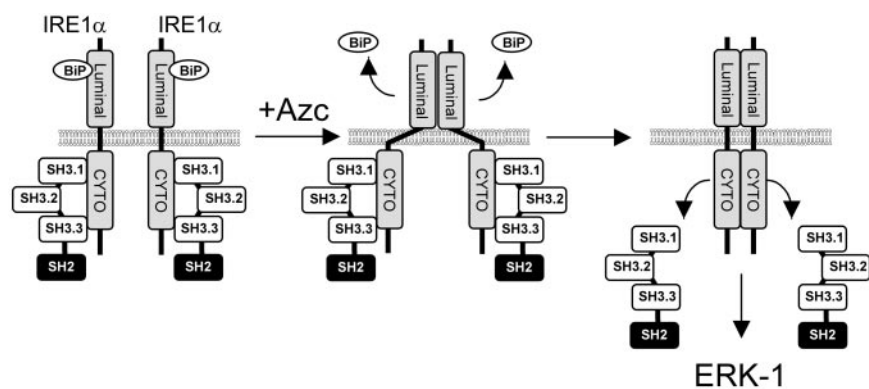


**Figure 9.** Proposed model for the regulation of ERK-1 activation by Nck upon Azc stress. Under basal conditions IRE1 associates with BiP within the lumen of the ER and with Nck SH3 domains in the cytosol to prevent IRE1 signaling. On Azc stress, misfolded proteins accumulate in the lumen of the ER and as a consequence BiP dissociates from IRE1. This induces the oligomerization of IRE1 luminal domains that possibly leads to conformational change of IRE1 cytosolic domain leading to the release of IRE1-bound Nck and subsequent IRE1-mediated activation of ERK-1.

cells and probably also for maintenance of basal ERK-1 activity. The 3SH3 domains of Nck-1 were sufficient to revert the immunodepletion effect (Figure 3C), thus indicating that the SH2 domain of Nck-1 was dispensable for ER stress-induced ERK-1 activation. In addition to promoting ERK-1 activation, Nck-1 prevented p38<sup>MAPK</sup> activation, thus suggesting a dual role for this adaptor. This may show a role for Nck-1 in buffering the equilibrium between the stress and/or proliferative pathways as reported previously by Roche *et al.* (1996). These data indicate a highly regulated balance between the SH2/SH3 scaffolding domains of Nck which, when disrupted, promotes either activation or inhibition of specific ER signaling pathways.

#### Negative Regulation of IRE1 Signaling by Nck

Experiments where Nck-1 was stably associated with the ER membrane showed both in vivo and in vitro that the ER stress-induced ERK-1 activation was abrogated (Figure 7, D and E). These observations could result from the fact that we created a negative mutant of IRE1 $\alpha$  and therefore blocked the signaling from this molecule similar to what is observed with a kinase-defective (K599AA) IRE1 $\alpha$  (Tirasophon *et al.*, 1998). This hypothesis was partly ruled out by the results obtained with a chimera containing the luminal and transmembrane domains of Trap $\alpha$  fused to Nck-1 (3SH3), which led to similar results to those obtained with the IRE1 $\alpha$ .Nck-1 construct (Figure 7, D and E). This suggested 1) that the effects observed with the IRE1 $\alpha$ .Nck-1 chimera was not completely due to a dominant negative effect and 2) that, similar to the repression of IRE1 signaling by binding of BiP in the lumen (Bertolotti *et al.*, 2000), the basal association of Nck with IRE1 may represent an inhibitory system to prevent IRE1 signaling. Such a Nck-dependent inhibitory system to prevent ER signaling is not restricted to IRE1 because Nck-1 also antagonizes signaling from PERK (Kebache *et al.*, 2004), an ER transmembrane kinase involved in the ER stress-induced attenuation of translation through phosphorylation of eIF2 $\alpha$  (Harding *et al.*, 1999; Bertolotti *et al.*, 2000). The negative role of Nck on cell signaling is further supported by the fact that Nck is also implicated in the attenuation of signals emanating from the plasma membrane (Jones and Dumont, 1999; Buday *et al.*, 2002; Murakami *et al.*, 2002).

Based on these results, we propose a model where under basal conditions, Nck is associated with IRE1, thereby preventing IRE1 signaling leakage. On Azc stress, IRE1 oligomerization and subsequent transphosphorylation may induce conformational change of the cytosolic domain and consequently promote a decrease in affinity for Nck, leading to its dissociation. We hypothesize that the dissociation of Nck from IRE1 exposes binding sites on IRE1 cytosolic do-

main for allowing the recruitment of intermediates of the MAPK signaling (Figure 9). In this model, IRE1 would serve as signaling scaffold to lead to ERK activation. Several intermediates of this pathway have already been shown to localize on the ER membrane such as ERK-1 (Chevet *et al.*, 1999b), mitogen-activated protein kinase kinase-1 (unpublished observations), and Ras (Chiu *et al.*, 2002), which suggests an ER proximal activation of this pathway mediated by IRE1.

#### Mechanism of Nck-mediated ERK-1 Activation

The above-mentioned model would explain the apparent discrepancies between the results shown in Figures 3C and 6B. Indeed, immuno-isolated ER membranes represent a snapshot of the signaling components present in the cell at a given time. Signaling events emerging from these membranes will come from 1) IRE-1 molecules that were activated during the induction of the stress in the cell and 2) de novo activation of IRE-1 molecules in vitro due to the presence of aggregates in the lumen of the ER that will not be resorbed. In the case of the immunodepletion, all of the cytosolic Nck molecules were removed from the cytosol, but there was still a fraction of Nck bound to IRE1; therefore, upon incubation of Azc-stressed microsomes purified from FR3T3 cells with immunodepleted cytosol, Nck molecules bound to IRE1 are released into the incubation medium, thereby allowing further IRE1 signaling and a slight but significant ERK-1 activation. This would explain why ERK-1 activity does not return to basal levels under these conditions (compare ctrl untreated and -Nck + Azc, Figure 3C). The presence of Nck in the cytosol would therefore be required for recycling to the ER membrane through binding to IRE-1 and to promote further signaling to ERK-1. Alternatively, when microsomes isolated from Nck-null cells are incubated with recombinant Nck-1, Nck-1 would bind to the Azc-stressed and nonstressed microsomes. However, because Azc-stressed microsomes are sensitized and competent to transduce IRE1 signaling, Nck dissociates from IRE1, thus allowing subsequent ERK-1 activation. This hypothesis would be consistent with the observation that less Nck-1 was found associated with Azc-stressed microsomes than with nonstressed microsomes, suggesting a dissociation of Nck from the ER membrane upon Azc stress. Conversely, in the absence of stress, microsomes are not competent for IRE1 signaling and Nck remains associated with IRE1, thus preventing its signaling and downstream ERK-1 activation. This negative regulatory mechanism of Nck toward IRE1-mediated ERK-1 activation is further supported by the 1.8-fold higher basal activity of ERK-1 in Nck<sup>-/-</sup> cells than in Nck<sup>+/+</sup> cells (Figure 8B). In this case, the negative regula-

tion of Azc-induced IRE1 signaling by ER-bound Nck would not take place in the Nck<sup>-/-</sup> cells, thus leading to a higher activation level of ERK-1 in the Nck-null cells and could explain the higher survival rate and lower apoptosis rate in these cells.

#### *Adaptative and Proapoptotic Balance Regulation by Nck during ER Stress*

Experiments where Nck<sup>+/+</sup> and Nck<sup>-/-</sup> MEFs were subjected to different Azc treatments showed no difference in the up-regulation of the UPR markers BiP and CHOP or in the up-regulation of XBP-1 transcription and subsequent splicing (Figure 8A). Although no detectable difference was observed in these cells for BiP induction in response to Azc, Kebache *et al.* (2004) have reported that overproduction of Nck-1 in human embryonic kidney cells impaired BiP induction upon thapsigargin treatment, suggesting that the Nck-dependent induction of BiP transcription could be stress specific.

Under Azc stress, the fact that ERK-1 was activated to a higher level in the Nck<sup>-/-</sup> cells than in the Nck<sup>+/+</sup> cells (Figure 8B) indicated that endogenous Nck negatively regulates ERK-1 activation. The higher activation of ERK-1 in Nck<sup>-/-</sup> cells upon Azc treatment correlated with their enhanced survival (1.5-fold increase after 12-h treatment compared with the Nck<sup>+/+</sup> cells, Figure 8C). When Nck<sup>+/+</sup> and Nck<sup>-/-</sup> MEFs were treated with Azc for 2 to 4 h, there was a significant increase in the percentage of apoptotic Nck<sup>+/+</sup> cells but no effect on the Nck<sup>-/-</sup> cells was observed (Figure 8E). This different behavior of Nck<sup>+/+</sup> and Nck<sup>-/-</sup> cells toward ER stress supports the findings that Nck-1 overproduction impairs cell survival in response to thapsigargin (Kebache *et al.*, 2004).

In conclusion, this is the first report of an ER stress-mediated activation of ERK-1. In addition, this mechanism is dependent on the adaptor molecule Nck-1, which to date, had only been described as mediating extracellular signals. These results were obtained through the establishment of a cell-free signaling assay in which we used immuno-isolated ER membranes from cells in culture, and cytosol from rat liver. Finally, our results delineate a novel mechanism for the regulation of ER stress signaling to the MAPK pathway and demonstrate a critical role for Nck during the Azc-induced ER stress response leading to ERK-1 activation and apoptosis. Overall, our data provide new insights into the current knowledge of ER stress-activated signaling pathways and may lead to a better understanding of the molecular mechanisms triggered by the cell to provide specificity in proteotoxicity signaling.

#### ACKNOWLEDGMENTS

We are grateful to J. Mui (McGill Electron Microscopy Center) and B. Giannias (Department of Surgery, McGill University) for technical assistance on electron microscopy pictures and fluorescence-activated cell sorting analysis, respectively. We thank P. H. Cameron, S. Palcy, P. Auguste and M. Park for critical reading of the manuscript. This work was mainly funded by a grant from the Canadian Institutes of Health Research (#MOP53357) and by startup funds from the Department of Surgery at McGill University to E.C., and by grants from the Canadian Diabetes Association to L.L., the NCIC to J.J.M.B., and the National Institutes of Health (#036594) to R.J. H.N.W. was supported by a postdoctoral fellowship from the FRSQ. E.L. was supported by a Genome Quebec grant to the Montreal Proteomic Network. S.J. was supported in part by a Genome Quebec grant to the Montreal Proteomic Network and a Canadian Institutes of Health Research postdoctoral fellowship. D.T.N. was supported in part by a postdoctoral fellowship from the MUHC-Research Institute. E.C. is supported by the Simone and Morris Fast foundation and a Chercheur-Boursier scholarship from the FRSQ.

#### REFERENCES

- Aridor, M., and Balch, W.E. (1999). Integration of endoplasmic reticulum signaling in health and disease. *Nat. Med.* 5, 745–751.
- Barbosa-Tessmann, I.P., Chen, C., Zhong, C., Schuster, S.M., Nick, H.S., and Kilberg, M.S. (1999). Activation of the unfolded protein response pathway induces human asparagine synthetase gene expression. *J. Biol. Chem.* 274, 31139–31144.
- Bell, A.W., *et al.* (2001). Proteomics characterization of abundant Golgi membrane proteins. *J. Biol. Chem.* 276, 5152–5165.
- Bertolotti, A., Zhang, Y., Hendershot, L.M., Harding, H.P., and Ron, D. (2000). Dynamic interaction of BiP and ER stress transducers in the unfolded-protein response. *Nat. Cell Biol.* 2, 326–332.
- Bork, P., and Sander, C. (1993). A hybrid protein kinase-RNase in an interferon-induced pathway? *FEBS Lett.* 334, 149–152.
- Brostrom, C.O., Prostko, C.R., Kaufman, R.J., and Brostrom, M.A. (1996). Inhibition of translational initiation by activators of the glucose-regulated stress protein and heat shock protein stress response systems. Role of the interferon-inducible double-stranded RNA-activated eukaryotic initiation factor 2alpha kinase. *J. Biol. Chem.* 271, 24995–25002.
- Buday, L. (1999). Membrane-targeting of signalling molecules by SH2/SH3 domain-containing adaptor proteins. *Biochim. Biophys. Acta* 1422, 187–204.
- Buday, L., Wunderlich, L., and Tamas, P. (2002). The Nck family of adapter proteins: regulators of actin cytoskeleton. *Cell Signal* 14, 723–731.
- Calfon, M., Zeng, H., Urano, F., Till, J.H., Hubbard, S.R., Harding, H.P., Clark, S.G., and Ron, D. (2002). IRE1 couples endoplasmic reticulum load to secretory capacity by processing the XBP-1 mRNA. *Nature* 415, 92–96.
- Chang, L., and Karin, M. (2001). Mammalian MAP kinase signalling cascades. *Nature* 410, 37–40.
- Chen, X., Shen, J., and Prywes, R. (2002). The luminal domain of ATF6 senses ER stress and causes translocation of ATF6 from the ER to the Golgi. *J. Biol. Chem.*
- Chevet, E., Lemaitre, G., Cailleret, K., Dahan, S., Bergeron, J.J., and Katinka, M.D. (1999a). Identification and characterization of an intracellular protein complex that binds fibroblast growth factor-2 in bovine brain. *Biochem. J.* 341, 713–723.
- Chevet, E., Wong, H.N., Gerber, D., Cochet, C., Fazel, A., Cameron, P.H., Gushue, J.N., Thomas, D.Y., and Bergeron, J.J. (1999b). Phosphorylation by CK2 and MAPK enhances calnexin association with ribosomes. *EMBO J.* 18, 3655–3666.
- Chiu, V.K., Bivona, T., Hach, A., Sajous, J.B., Silletti, J., Wiener, H., Johnson, R.L., 2nd, Cox, A.D., and Phillips, M.R. (2002). Ras signalling on the endoplasmic reticulum and the Golgi. *Nat. Cell Biol.* 4, 343–350.
- Di Guglielmo, G.M., Baass, P.C., Ou, W.J., Posner, B.I., and Bergeron, J.J. (1994). Compartmentalization of SHC, GRB2 and mSOS, and hyperphosphorylation of Raf-1 by EGF but not insulin in liver parenchyma. *EMBO J.* 13, 4269–4277.
- Ellgaard, L., and Helenius, A. (2003). Quality control in the endoplasmic reticulum. *Nat. Rev. Mol. Cell. Biol.* 4, 181–191.
- Fons, R.D., Bogert, B.A., and Hegde, R.S. (2003). Substrate-specific function of the translocon-associated protein complex during translocation across the ER membrane. *J. Cell Biol.* 160, 529–539.
- Gruenberg, J., and Howell, K.E. (1985). Immuno-isolation of vesicles using antigenic sites either located on the cytoplasmic or the exoplasmic domain of an implanted viral protein. A quantitative analysis. *Eur. J. Cell Biol.* 38, 312–321.
- Gruenberg, J.E., and Howell, K.E. (1986). Reconstitution of vesicle fusions occurring in endocytosis with a cell-free system. *EMBO J.* 5, 3091–3101.
- Gruenheid, S., DeVinney, R., Bladt, F., Goosney, D., Gekop, S., Gish, G.D., Pawson, T., and Finlay, B.B. (2001). Enteropathogenic *E. coli* Tir binds Nck to initiate actin pedestal formation in host cells. *Nat. Cell Biol.* 3, 856–859.
- Hampton, R.Y. (2000). ER stress response: getting the UPR hand on misfolded proteins. *Curr. Biol.* 10, R518–R521.
- Harding, H.P., Zhang, Y., and Ron, D. (1999). Protein translation and folding are coupled by an endoplasmic-reticulum-resident kinase [correction published in published in *Nature* (1999) 398, 90]. *Nature* 397, 271–274.
- Haze, K., Yoshida, H., Yanagi, H., Yura, T., and Mori, K. (1999). Mammalian transcription factor ATF6 is synthesized as a transmembrane protein and activated by proteolysis in response to endoplasmic reticulum stress. *Mol. Biol. Cell* 10, 3787–3799.
- Hazzalin, C.A., and Mahadevan, L.C. (2002). MAPK-regulated transcription: a continuously variable gene switch? *Nat. Rev. Mol. Cell. Biol.* 3, 30–40.

- High, S., Lecomte, F.J., Russell, S.J., Abell, B.M., and Oliver, J.D. (2000). Glycoprotein folding in the endoplasmic reticulum: a tale of three chaperones? *FEBS Lett.* *476*, 38–41.
- Johnson, G.L., and Lapadat, R. (2002). Mitogen-activated protein kinase pathways mediated by ERK, JNK, and p38 protein kinases. *Science* *298*, 1911–1912.
- Jones, N., and Dumont, D.J. (1999). Recruitment of Dok-R to the EGF receptor through its PTB domain is required for attenuation of Erk MAP kinase activation. *Curr. Biol.* *9*, 1057–1060.
- Kaufman, R.J. (1999). Stress signaling from the lumen of the endoplasmic reticulum: coordination of gene transcriptional and translational controls. *Genes Dev.* *13*, 1211–1233.
- Kaufman, R.J., Scheuner, D., Schroder, M., Shen, X., Lee, K., Liu, C.Y., and Arnold, S.M. (2002). The unfolded protein response in nutrient sensing and differentiation. *Nat. Rev. Mol. Cell Biol.* *3*, 411–421.
- Kebache, S., Cardin, E., Nguyen, D.T., Chevet, E., and Larose, L. (2004). Nck-1 antagonizes the endoplasmic reticulum stress-induced inhibition of translation. *J. Biol. Chem.* *279*, 9662–9671.
- Kebache, S., Zuo, D., Chevet, E., and Larose, L. (2002). Modulation of protein translation by Nck-1. *Proc. Natl. Acad. Sci. USA* *99*, 5406–5411.
- Lavoie, C., Chevet, E., Roy, L., Tonks, N.K., Fazel, A., Posner, B.I., Paiement, J., and Bergeron, J.J. (2000). Tyrosine phosphorylation of p97 regulates transitional endoplasmic reticulum assembly in vitro. *Proc. Natl. Acad. Sci. USA* *97*, 13637–13642.
- Lee, K., Tirasophon, W., Shen, X., Michalak, M., Prywes, R., Okada, T., Yoshida, H., Mori, K., and Kaufman, R.J. (2002). IRE1-mediated unconventional mRNA splicing and S2P-mediated ATF6 cleavage merge to regulate XBP1 in signaling the unfolded protein response. *Genes Dev.* *16*, 452–466.
- Lin, C.C., Love, H.D., Gushue, J.N., Bergeron, J.J., and Ostermann, J. (1999). ER/Golgi intermediates acquire Golgi enzymes by brefeldin A-sensitive retrograde transport in vitro. *J. Cell Biol.* *147*, 1457–1472.
- Lotti, L.V., Lanfrancone, L., Migliaccio, E., Zompetta, C., Pellicci, G., Salcini, A.E., Falini, B., Pellicci, P.G., and Torrisi, M.R. (1996). Sch proteins are localized on endoplasmic reticulum membranes and are redistributed after tyrosine kinase receptor activation. *Mol. Cell Biol.* *16*, 1946–1954.
- Luers, G.H., Hartig, R., Mohr, H., Hausmann, M., Fahimi, H.D., Cremer, C., and Volkl, A. (1998). Immuno-isolation of highly purified peroxisomes using magnetic beads and continuous immunomagnetic sorting. *Electrophoresis* *19*, 1205–1210.
- Luo, S., and Lee, A.S. (2002). Requirement of the p38 mitogen-activated protein kinase signalling pathway for the induction of the 78 kDa glucose-regulated protein/immunoglobulin heavy-chain binding protein by azetidine stress: activating transcription factor 6 as a target for stress-induced phosphorylation. *Biochem J.* *366* (Pt 3), 787–795.
- Lussier, G., and Larose, L. (1997). A casein kinase I activity is constitutively associated with Nck. *J. Biol. Chem.* *272*, 2688–2694.
- Mengesdorf, T., Althausen, S., and Paschen, W. (2002). Genes associated with pro-apoptotic and protective mechanisms are affected differently on exposure of neuronal cell cultures to arsenite. No indication for endoplasmic reticulum stress despite activation of grp78 and gadd153 expression. *Brain Res. Mol. Brain Res.* *104*, 227–239.
- Morrison, D.K., and Davis, R.J. (2003). Regulation of MAP kinase signaling modules by scaffold proteins in mammals. *Annu. Rev. Cell Dev. Biol.* *19*, 91–118.
- Murakami, H., Yamamura, Y., Shimono, Y., Kawai, K., Kurokawa, K., and Takahashi, M. (2002). Role of Dok1 in cell signaling mediated by RET tyrosine kinase. *J. Biol. Chem.* *277*, 32781–32790.
- Nelson, D.S., Alvarez, C., Gao, Y.S., Garcia-Mata, R., Fialkowski, E., and Sztul, E. (1998). The membrane transport factor TAP/p115 cycles between the Golgi and earlier secretory compartments and contains distinct domains required for its localization and function. *J. Cell Biol.* *143*, 319–331.
- Nishitoh, H., Matsuzawa, A., Tobiume, K., Saegusa, K., Takeda, K., Inoue, K., Hori, S., Kakizuka, A., and Ichijo, H. (2002). ASK1 is essential for endoplasmic reticulum stress-induced neuronal cell death triggered by expanded polyglutamine repeats. *Genes Dev.* *16*, 1345–1355.
- Pawson, T., and Saxton, T.M. (1999). Signaling networks—do all roads lead to the same genes? *Cell* *97*, 675–678.
- Roche, S., McGlade, J., Jones, M., Gish, G.D., Pawson, T., and Courtneidge, S.A. (1996). Requirement of phospholipase C gamma, the tyrosine phosphatase Syp and the adaptor proteins Shc and Nck for PDGF-induced DNA synthesis: evidence for the existence of Ras-dependent and Ras-independent pathways. *EMBO J.* *15*, 4940–4948.
- Schrag, J.D., Procopio, D.O., Cygler, M., Thomas, D.Y., and Bergeron, J.J. (2003). Lectin control of protein folding and sorting in the secretory pathway. *Trends Biochem. Sci.* *28*, 49–57.
- Shen, X., *et al.* (2001). Complementary signaling pathways regulate the unfolded protein response and are required for *C. elegans* development. *Cell* *107*, 893–903.
- Tirasophon, W., Welihinda, A.A., and Kaufman, R.J. (1998). A stress response pathway from the endoplasmic reticulum to the nucleus requires a novel bifunctional protein kinase/endoribonuclease (Ire1p) in mammalian cells. *Genes Dev.* *12*, 1812–1824.
- Urano, F., Bertolotti, A., and Ron, D. (2000a). IRE1 and efferent signaling from the endoplasmic reticulum. *J. Cell Sci.* *113*, 3697–3702.
- Urano, F., Wang, X., Bertolotti, A., Zhang, Y., Chung, P., Harding, H.P., and Ron, D. (2000b). Coupling of stress in the ER to activation of JNK protein kinases by transmembrane protein kinase IRE1. *Science* *287*, 664–666.
- Wada, T., and Penninger, J.M. (2004). Mitogen-activated protein kinases in apoptosis regulation. *Oncogene* *23*, 2838–2849.
- Wang, X.Z., Kuroda, M., Sok, J., Batchvarova, N., Kimmel, R., Chung, P., Zinsner, H., and Ron, D. (1998). Identification of novel stress-induced genes downstream of chop. *EMBO J.* *17*, 3619–3630.
- Yoshida, H., Matsui, T., Hosokawa, N., Kaufman, R.J., Nagata, K., and Mori, K. (2003). A time-dependent phase shift in the mammalian unfolded protein response. *Dev. Cell* *4*, 265–271.
- Yoshida, H., Matsui, T., Yamamoto, A., Okada, T., and Mori, K. (2001). XBP1 mRNA is induced by ATF6 and spliced by IRE1 in response to ER stress to produce a highly active transcription factor. *Cell* *107*, 881–891.
- Zhang, K., and Kaufman, R.J. (2004). Signaling the unfolded protein response from the endoplasmic reticulum. *J. Biol. Chem.* *279*, 25935–25938.